Reflection-antisymmetric spatiotemporal chaos under field-translational invariance

Miki Y. Matsuo[1,2,*] and Masaki Sano[1]

[1]*Department of Physics, The University of Tokyo, Hongo, Bunkyo-ku, Tokyo, Japan*

[2]*Institute for Research on Earth Evolution, Japan Agency for Marine-Earth Science and Technology (JAMSTEC), Kanazawa-ku, Yokohama, Japan*

(Received 22 January 2011; revised manuscript received 24 October 2011; published 23 March 2012)

We propose a route to spatiotemporal chaos, in which the system is assumed to have spatial reflection antisymmetry and field-translation symmetry. The lowest-order nonlinear equation that satisfies these symmetries is explored with the weak nonlinear analysis around the bifurcation point. We conclude that the nonlinear term $\partial_x^2 u \partial_x^3 u$ is important to make a nontrivial dynamics, and show that the nonlinear dynamical equation having this term produces a turbulent dynamics.

DOI: 10.1103/PhysRevE.85.036215 PACS number(s): 05.45.Jn, 47.52.+j, 47.20.Ky, 47.20.Lz

I. INTRODUCTION

The route to spatiotemporal chaos and turbulence in a spatially extended system has been explored for a long time. Spatially extended oscillatory nonlinear systems show the simplest route to spatiotemporal chaos, in which the uniform oscillatory state becomes unstable against long-wavelength modulation via the Benjamin-Feir instability [1]. The steady convective flow is also noticed to be a possible origin of a transition to phase and defect chaos [2]. Understanding the turbulence in a nematic liquid crystal or Rayleigh-Benard (RB) convection proved considerably difficult, because of the symmetry constraints [3]. To understand the origin of spatiotemporal chaos in nonoscillatory systems, many studies noted the importance of mean flow effects due to long-wavelength deformation of a periodic structure in two or higher dimensions [4]. Sasa and Kaiser *et al.* independently showed that the nonlocal drift creates the zigzag instability that continues to cause turbulence [5–7]. On the other hand, many recent studies for amplitude and phase dynamics are concerned with the nonlocally extended systems beyond the local descriptions [8–17].

Among the various models that generate spatiotemporal chaos, the Kuramoto-Sivashinsky (KS) equation is well known as the simplest equation [1,18]. The KS equation is described by the two forms, $\partial_t u = -\partial_x^2 u - \partial_x^4 u - (\partial_x u)^2$ and $\partial_t v = -\partial_x^2 v - \partial_x^4 v - v\partial_x v$, which are mutually transformed by $v = \sqrt{2}u_x$. Although these two forms of the KS equation are mathematically equivalent, they are not physically equivalent because they have different symmetries. The first form is invariant against the two operations: the arbitrary translation of the scalar field, $u \to u + \text{const}$, and the spatial reflection, $x \to -x$. On the other hand, the latter form is invariant against spatial antisymmetric transformation, $x \to -x$ and $v \to -v$, but it is variant against translation of the scalar field. Several equations that produce spatiotemporal chaos have been proposed until now, such as the Benny equation [19], the Kolmogorov-Spiegel-Sivashinsky equation [20], and the Nikolaevskii equation [21,22], each of which satisfies one of the symmetries mentioned above for the KS equation. If a system does not satisfy one of the symmetries, for example, the system is invariant against the spatial reflection and the translation of the scalar field then the spatiotemporal chaos becomes hard to be realized. This is the reason why it has been hard to understand the turbulence in a nematic liquid crystal or RB convection, in which the system is invariant against the arbitrary translation and the spatial reflection when the system is around the critical point [5–7]. This leads to the question: Is there any simple mechanism that shows spatiotemporal chaos without the symmetries that the KS equation satisfies? This question is quite important when considering rotationally symmetric spatially extended systems that do not have oscillatory instability because these systems are not in the range of application of the KS equation. In fact, it is known that spatiotemporal disturbance appears in homeotropic nematics, where disturbance suddenly arises from a spatially uniform state without oscillatory instability [23–25]. Thus, in this paper, we explore the further possibility of producing spatiotemporal chaos without the symmetries that the KS equation satisfies, and, hence, we propose an alternate route to spatiotemporal chaos.

II. LONG WAVELENGTH EXPANSION

Let us consider a one-dimensional scalar field $u(x,t)$, whose dynamics is described by

$$\partial_t u = f_\mu(u), \tag{1}$$

where μ is the bifurcation parameter. We assume that this equation has a trivial solution $u = 0$, which is stable for $\mu < \mu_c$, while the solution becomes unstable beyond the critical value $\mu = \mu_c$. Now, we assume that the bifurcation parameter is sufficiently close to the critical value. To consider the general weak nonlinear description, we further assume that only the long-wavelength mode becomes unstable beyond the critical value. Because u is sufficiently long waved, we can approximate the right-hand side of Eq. (1) by the function Ω, which includes only the low-order local derivatives,

$$f_\mu(u) = \Omega_\mu\left(u, \partial_x u, \partial_x^2 u, \ldots, \partial_x^m u\right) + O(\varepsilon^2), \tag{2}$$

where the parameter ε is defined by $\varepsilon = \mu/\mu_c - 1$, and m is some integer. Now, we expand Ω with low-order arguments, expecting that a self-sustained description of the slow long-wavelength mode is possible around the critical

*mikiy@jamstec.go.jp

point. To determine the leading terms of the expansion, we must select only the low-order terms satisfying the symmetry constraint. Here we assume the following two invariances: i) Ω is independent of u, and ii) Ω is invariant with respect to the simultaneous transformations $x \to -x$ and $u \to -u$. Selecting the $O(u^2)$ terms from the expansion satisfying these symmetry conditions, we obtain

$$u_t = \epsilon_2 \partial_x^2 u - \epsilon_4 \partial_x^4 u + \epsilon_6 \partial_x^6 u - \cdots + g_1 \partial_x u \partial_x^2 u + g_2 \partial_x^2 u \partial_x^3 u + g_3 \partial_x u \partial_x^4 u + \cdots. \quad (3)$$

The parameters ϵ_i are determined by the expansion of the eigenvalue spectrum $\lambda(k) \simeq -\epsilon_2 k^2 - \epsilon_4 k^4 - \epsilon_6 k^6 - \cdots$ calculated by the linear stability analysis of the original equation (1). The effective nonlinear equation for the case that $\epsilon_2 \partial_x^2 u$ is the main destabilizing term, that is, $\epsilon_2 \to -0$ and $\epsilon_i > 0 (i \geqslant 4)$ was studied by Kuramoto, with which he discussed the spontaneous wavelength modulation of a periodic pattern [26]. In this paper, to explore the further possibility, we consider the case that the main destabilizing term is the quartic diffusion term $\epsilon_4 \partial_x^4 u$. When we interpret the linear terms in the sense of nonconservative surface, each linear term is interpreted as surface tension, bending rigidity, and higher-order rigidity. While we should assume that the quartic term means surface tension, the sextic term means bending rigidity, and the quadratic term should be zero in the case of conservative surface. Therefore, when we assume a nonconservative surface, the destabilization expressed by $\epsilon_4 < 0$ corresponds to generation of a negative bending rigidity, while Kuramoto's situation corresponds to generation of a negative surface tension.

When the quartic diffusion term is the main destabilizing term, we should consider the limit, $\epsilon_2 \to +0$ and $\epsilon_4 \to -0$. However, this limit is not unique but depends on the convergence rates. To determine the well-defined limit, we assume the scaling relation $|\epsilon_2| \sim c\epsilon^\nu$, where $\epsilon \equiv |\epsilon_4|$ and c is a small constant. Now, we remember the fact that the parameter ϵ describes a small shift from the bifurcation point. Due to its small value, we expect that the solution u has a

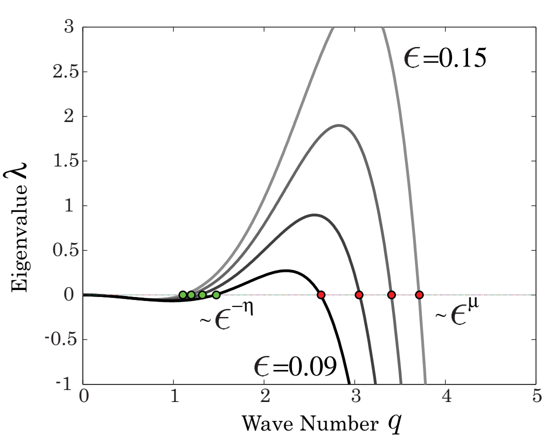

FIG. 1. (Color online) Transition of the eigenvalue spectrum, $\lambda = -0.3\epsilon^\nu q^2 + \epsilon q^4 - 0.01 q^6$. Here, the value of the exponent ν is set to $\nu = 0.3$. Solid lines are eigenvalue spectrums for $\epsilon = 0.15, 0.13, 0.11$, and 0.09, in which the darker line is obtained when the value of ϵ is smaller.

scaling form, although we must take note of the fact that the system should have multiple scales (see Fig. 1). Let us assume that the system has a characteristic length scale $1/q^*$ in the limit $\epsilon \to 0$, which distinguishes the scaling behaviors of the solution. The solution u is assumed to have the scaling forms as $u = u(\epsilon^{-\eta} x)$ when $q < q^*$ and $u = u(\epsilon^{\mu} x)$ when $q > q^*$. The scaling parameters η and μ are determined by the balances between the quadratic and quartic diffusion terms and between the quartic and sextic diffusion terms in Eq. (3), which leads to $\eta = (1-\nu)/2$ and $\mu = 1/2$. When the solution has these scalings, the derivative $\partial_x^n u$ is expected to scale as $\partial_x^n u \sim \epsilon^{-\eta n} u$ when $n < n^*$, and scale as $\partial_x^n u \sim \epsilon^{-\eta n^* + \mu(n-n^*)} u$ when $n \geqslant n^*$, where n^* is some critical order, which should be $n^* = 3 \sim 5$ when the destabilizing term is quartic. Now, we restrict our attention to the lowest-order effective description for $q^* < q$, which is equivalent to ignoring the second-order linear term. Moreover, when $\epsilon \to 0$, the linear terms including high derivatives are ignored. To select the most effective nonlinear term, we consider how each nonlinear term in Eq. (3) scales. For example, when we assume that $n^* = 3$, the nonlinear terms scale as $\partial_x u \partial_x^2 u \sim \epsilon^{-3\eta}, \partial_x^2 u \partial_x^3 u \sim \epsilon^{-5\eta}, \partial_x u \partial_x^4 u \sim \epsilon^{-4\eta+\mu}$, and $\partial_x^3 u \partial_x^4 u \sim \epsilon^{-6\eta+\mu}$, from which we can determine the most effective term depending on the value of ν.

As the first example, we consider the case $\nu < 0$. In this case, we see the most effective nonlinear term is $\partial_x u \partial_x^2 u$, and, therefore, the lowest-order equation is

$$u_t = \partial_x^4 u + \partial_x^6 u + \partial_x u \partial_x^2 u, \quad (4)$$

where we eliminated the parameters, ϵ, ϵ_6, and g_1, considering the adequate scalings of the variables. Although Eq. (4) is somewhat different, it is not so attractive, because the solution of Eq. (4) does not display a complex behavior. This is understood by the fact that Eq. (4) has the Lyapunov functional $\mathcal{F}$ defined by

$$\partial_t u = -\delta \mathcal{F}/\delta u, \quad (5)$$

$$\mathcal{F} = \frac{1}{2} \int dx \left(-\left(\partial_x^2 u\right)^2 + \left(\partial_x^3 u\right)^2 + \frac{1}{3}(\partial_x u)^3 \right), \quad (6)$$

which characterizes the inevitable relaxation to some steady state. By the numerical simulation of Eq. (4), we see that the system shows the steady wave pattern.

When we consider the other value of ν, we get the other effective description. When we consider the case $0 < \nu < 1/2$, the second nonlinear term in Eq. (3) becomes the most effective, which leads to

$$u_t = \partial_x^4 u + \partial_x^6 u - \partial_x^2 u \partial_x^3 u, \quad (7)$$

where we eliminated the parameters again, considering the adequate scalings. The selection of the negative sign of the third term of the right-hand side is more appropriate when explaining the origin of the disturbed dynamics given later. Compared with the previous nonlinear term, the term $\partial_x^2 u \partial_x^3 u$ has a quite irrelevant effect in the dynamics, and one of the reasons is that this term does not have a potential function. We propose that this equation is important when considering spatiotemporal chaos under the reflection-antisymmetric condition.

III. NUMERICAL INVESTIGATIONS

Now, we investigate Eq. (7) by direct numerical calculations. In our numerical calculations, we use the exponential time-differencing fourth-order Runge-Kutta method (ETDRK4) to solve the equation [28,29]. The ETD methods are effective to rapidly and reliably solve a stiff equation like Eq. (7) because the error does not depend on the magnitude of the eigenvalues of the linear operator [28]. The ETDRK4 used here is the stabilized version developed by Kassam and Trefethen [29], which was verified to work well to solve the Kuramoto-Sivashinsky equation. Figure 2 shows various dynamical patterns obtained by solving Eq. (7) on several values of the system size L. Figure 2(a) shows one of the spatiotemporal patterns obtained by solving Eq. (7), in which the system shows a steady mode-2 wave. This kind of steady pattern is seen in a broad range of the value of the parameter L, although the stable wave mode changes depending on the value of L. This property is similar to that of the KS equation [18]. The dynamics becomes highly diverse in the three characteristic parameter windows, W_1, W_2, and W_3, each of which is defined by $L \simeq [12.0,14.4],[21.0,21.9]$, and $[29.0,29.9]$. The reason these windows are important is explained later. Figure 2(b) shows the traveling wave solution obtained in the first window W_1. The heteroclinic oscillation shown in Fig. 2(c) is also seen in the first window. Figure 2(d) shows the other heteroclinic oscillation, which is obtained in W_3. The further complex behavior as shown in Fig. 2(e) is obtained within W_2, in which the system shows the turbulent dynamics that never relaxes to a steady state. The property of this turbulent dynamics is analyzed by the power spectrum shown in Fig. 3. Figure 3(a) shows the time-averaged power spectrum $\langle S_n\rangle$ defined by $\langle S_n\rangle = \frac{1}{T}\int_{-\frac{T}{2}}^{\frac{T}{2}} dt|u_n(t)|^2$, where $u_n(t) = \frac{1}{L}\int_{-\frac{L}{2}}^{\frac{L}{2}} dx\,u(x,t)\exp(i\frac{2\pi n}{L}x)$ and T is the whole observation time. The exponential decay in the spectrum implies that the temporal development of the solution is spatiotemporal chaos [18,27]. Figure 3(b) shows the frequency spectrum for several low modes. All the modes show power-law decays whose slopes are -2, which implies that the dynamics is random.

To explain why Eq. (7) can generate the complex behavior in more detail, we give the Fourier expansion of u, $u = i\sum a_n \exp(2\pi i n s/L)$. Substituting this into Eq. (7), we get the mode interaction equations as

$$\dot{a}_n = n^4\left(1 - \frac{n^2}{\Lambda^2}\right)a_n + \sum_{m=-\infty}^{m=\infty} m^2 (n-m)^3 a_m a_{n-m}, \qquad (8)$$

where Λ is defined by $\Lambda \equiv L/2\pi$, we performed the scale transformations $t \to \Lambda^4 t$ and $a_n \to \Lambda a_n$, and we used the fact that $a_{-n} = -a_n^*$ should be satisfied, when u is real valued. Equation (8) shows that the mode-n wave a_n becomes unstable at $L \sim 2\pi n$, from which we see that each window W_1, W_2, and W_3 is in the neighborhood of the parameter value that the mode-2, mode-3, and mode-4 becomes unstable, respectively. The high codimension bifurcation points exist within these windows, and, therefore, the various changes of motion type can appear [30]. Now, we analyze the effective dynamics in W_2, in which the system generates spatiotemporal disturbances. Because the three modes a_1,a_2, and a_3 are unstable or neutrally stable in W_2, the slow dynamics in W_2 is determined by the center-unstable manifold spanned by (a_1,a_2,a_3). The dynamics on the center-unstable manifold can be calculated with the

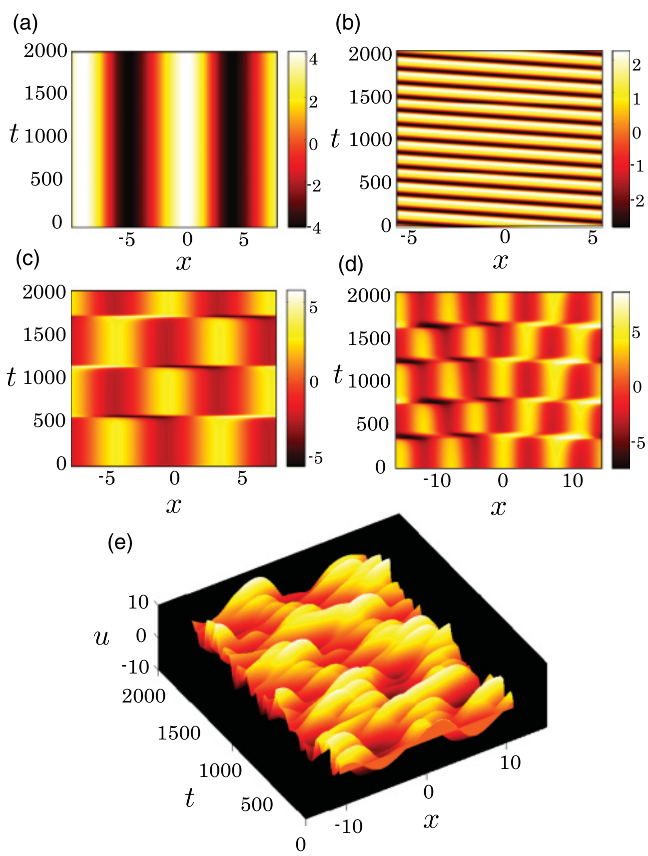

FIG. 2. (Color online) Spatio-temporal dynamics of the solution of Eq. (7). (a) Steady wave ($L = 18.0$). (b) Traveling wave ($L = 12.5$). (c) Heteroclinic oscillation ($L = 13.7$). (d) Heteroclinic oscillation ($L = 29.5$). (e) Turbulized dynamics ($L = 21.5$). Here, we use the spectral algorithm with a fourth order exponential time differencing Runge-Kutta method (ETDRK4) [29], where the whole mode number is $N = 512$.

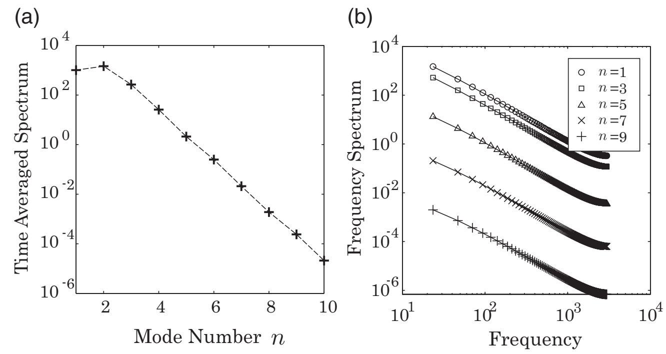

FIG. 3. (a) Time-averaged power spectrum. The spectrum higher than the $n = 10$ mode continues to exponentially decrease (not shown here). (b) Frequency spectrum of low-wavenumber modes: $n = 1,3,5,7$, and 9. These are obtained by numerically solving Eq. (7) with the same parameter values as those used in Fig. 2(e).

standard center manifold reduction technique [30], which leads to

$$\dot{a}_1 = \Lambda_1 a_1 - 4a_2 a_1^* - 36a_3 a_2^* + D_1 a_1 |a_3|^2 + D_2 a_2^2 a_3^* + O(|a|^4), \quad (9)$$

$$\dot{a}_2 = \Lambda_2 a_2 + a_1^2 - 18a_3 a_1^* + D_3 a_3 a_1 a_2^* + D_4 a_2 |a_2|^2 + D_5 a_2 |a_3|^2 + O|a|^4), \quad (10)$$

$$\dot{a}_3 = \Lambda_3 a_3 + 12a_1 a_2 + D_6 a_3 |a_1|^2 + D_7 a_2^2 a_1^* + D_8 a_3 |a_2|^2 + D_9 a_3 |a_3|^2 + O(|a|^4), \quad (11)$$

where $\Lambda_n = n^4(1 - n^2/\Lambda^2)$, and the $O(|a|^3)$ coefficients are given by $D_1 = -20736/(\Lambda_1 + \Lambda_3 - \Lambda_4), D_2 = -18432/(\Lambda_2 - \Lambda_4)$, $D_3 = -9216/(\Lambda_1 + \Lambda_3 - \Lambda_4)$, $D_4 = -8192/(\Lambda_2 - \Lambda_4), D_5 = -202500/(\Lambda_2 + \Lambda_3 - \Lambda_5)$, $D_6 = -2304/(\Lambda_1 + \Lambda_3 - \Lambda_4)$, $D_7 = -2048/(\Lambda_2 - \Lambda_4)$, $D_8 = -90000/(\Lambda_2 + \Lambda_3 - \Lambda_5)$, and $D_9 = -472\,392/(\Lambda_3 - \Lambda_6)$. Here, we notice that the coefficient of the nonlinear term $a_2 a_1^*$ in Eq. (9) is negative and the coefficient of the term a_1^2 in Eq. (10) is positive. These properties have a significant role in these mode equations, because they imply that the system is able to produce the heteroclinic bifurcation [31]. This fact was indicated by Armbruster *et al.*, who provided the detailed bifurcation analysis of the equations similar to Eqs. (9) and (10) with $a_3 = 0$ [31]. Their pioneering work is helpful to understand how Eq. (7) produces a complex behavior in W_2, where it could be expected that the heteroclinic orbit perturbed by Eq. (11) generates the Smale's horseshoe structure [32]. In order to consider the dynamics within W_3, we have to treat the center-unstable manifold spanned by (a_1,a_2,a_3,a_4) near $\mu^2 = 16$ using the same technique, which should clarify the other heteroclinic orbit.

Here, we remark on the importance of the nonlinear term $\partial_x^2 u \partial_x^3 u$ from the viewpoint of nonlocality. As seen before, this term is essential for the realization of the turbulent dynamics displayed in Fig. 2(e). So far, the importance of the $\partial_x^2 u \partial_x^3 u$ term has not been noticed, probably because it does not have a significant effect due to the presence of high-order derivatives. This opinion is appropriate as long as the second-order linear term is the main destabilizing term. To maintain this mathematical structure, the derivatives included in the nonlinear terms should be at most second order and, hence, the $\partial_x^2 u \partial_x^3 u$ term must be excluded. However, in the case that the quartic derivative term is the main destabilizing term, we must consider the nonlinear terms including at most $\partial_x^4 u$, thus, the $\partial_x^2 u \partial_x^3 u$ term can appear in the lowest-order equation. Therefore, the importance of the $\partial_x^2 u \partial_x^3 u$ term manifests when we consider nonlocal systems. In the last decade, it has been identified that certain important aspects of the nonlocal reaction-diffusion models are never realized by the local amplitude and phase equations [8–14]. For instance, the complex Ginzburg-Landau (CGL) equation with exponential nonlocal coupling shows a multiaffine fractal structure [8,9]. The nonlocally coupled phase oscillators show pattern shredding, phase slips, and a chimera state [15], while the nonlocal oscillators having two coupling ranges display phase turbulence [16]. Although it is not clear how these preceding studies are related to our work, we consider that our findings develop the study of spatiotemporal chaos and nonlocal systems.

IV. CONCLUSION

In this paper, we proposed a route to spatiotemporal chaos. We considered the system that has space-reflection antisymmetry and field-translation symmetry. We conclude that Eq. (7) is the lowest-order equation that can show nontrivial turbulent dynamics within the symmetry constraint. Because the symmetry constraint assumed in this paper is very common in spatially extended physical systems, we believe that this scenario can universally describe the disturbance of many physical systems. We hope this study becomes a catalyst for creating a unified picture of various systems that show turbulent dynamics.

ACKNOWLEDGMENT

We appreciate Y. Kuramoto and T. Ohta for helpful comments.

[1] Y. Kuramoto, *Chemical Oscillations, Waves, and Turbulence* (Springer, Berlin, 1984).
[2] N. Garnier, A. Chiffaudel, and F. Daviaud, Phys. Rev. Lett. **88**, 134501 (2002).
[3] H. S. Greenside and M. C. Cross, Phys. Rev. A **31**, 2492 (1985).
[4] P. Manneville, *Dissipative Structures and Weak Turbulence*, (Academic Press, San Diego, 1990).
[5] S. Sasa, Prog. Theor. Phys. **83**, 824 (1990); **84**, 1009 (1990).
[6] M. Kaiser, W. Pesch, and E. Bodenschatz, Physica D **59**, 320 (1992).
[7] M. Kaiser and W. Pesch, Phys. Rev. E **48**, 4510 (1993).
[8] Y. Kuramoto, Prog. Theor. Phys. **94**, 321 (1995).
[9] Y. Kuramoto, D. Battogtokh, and H. Nakao, Phys. Rev. Lett. **81**, 3543 (1998).
[10] D. Tanaka and Y. Kuramoto, Phys. Rev. E **68**, 026219 (2003).
[11] L. Gelens, D. Gomila, G. Van der Sande, M. A. Matias, and P. Colet, Phys. Rev. Lett. **104**, 154101 (2010).
[12] N. Mazouz, G. Flatgen, and K. Krischer, Phys. Rev. E **55**, 2260 (1997).
[13] H. Varela, C. Beta, A. Bonnefont, and K. Krischer, Phys. Rev. Lett. **94**, 174104 (2005).
[14] V. Garcia-Morales and K. Krischer, Phys. Rev. Lett. **100**, 054101 (2008).
[15] D. M. Abrams, R. Mirollo, S. H. Strogatz, and D. A. Wiley, Phys. Rev. Lett. **101**, 084103 (2008).
[16] D. Battogtokh, Phys. Lett. A **299**, 558 (2002).
[17] P. C. Bressloff and Z. P. Kilpatrick, Phys. Rev. E **78**, 041916 (2008).
[18] J. M. Hyman and B. Nicolaenko, Physica D **18**, 113 (1986).
[19] D. J. Benny, Stud. Appl. Math. **L11**, 45 (1973).
[20] M. C. Depassier and E. A. Spiegel, Astron. J. **86**, 496 (1981).

[21] V. N. Nikolaevskii, in *Recent Advances in Engineering Science*, edited by S. L. Koh and C. G. Speciale, Lecture Notes in Engineering, No. 39 (Springer, Berlin, 1989).

[22] M. I. Tribelsky and K. Tsuboi, Phys. Rev. Lett. **76**, 1631 (1996).

[23] Y. Hidaka, J.-H. Huh, K. I. Hayashi, S. Kai, and M. I. Tribelsky, Phys. Rev. E **56**, 6256 (1997).

[24] R. Anugraha, Y. Hidaka, T. Ueki, and S. Kai, Phys. Rev. E **80**, 041701 (2009).

[25] F. Nugroho, T. Ueki, R. Anugraha, Y. Hidaka, and S. Kai, Phys. Rev. E **84**, 011709 (2011).

[26] Y. Kuramoto, Prog. Theor. Phys. **71**, 1182 (1984).

[27] P. Manneville, Phys. Lett. A **84**, 129 (1981).

[28] S. M. Cox and P. C. Matthews, J. Comp. Phys. **176**, 430 (2002).

[29] A. Kassam and L. N. Trefethen, SIAM J. Sci. Comput. **26**, 1214 (2005).

[30] S. Wiggins, *Introduction to Applied Nonlinear Dynamical Systems and Chaos* (Springer, Berlin, 2003).

[31] D. Armbruster, J. Gukenheimer, and P. Holmes, Physica D **29**, 257 (1988).

[32] E. Otto, *Chaos in Dynamical Systems* (Cambridge University Press, Cambridge, 2002).